Organic & Biomolecular Chemistry

Cite this: *Org. Biomol. Chem.*, 2011, **9**, 3549

www.rsc.org/obc

PAPER

Photoswitchable rotaxanes on gold nanoparticles†

Yingxin Duo, Sabine Jacob and Werner Abraham*

Received 24th January 2011, Accepted 28th February 2011
DOI: 10.1039/c1ob05128h

We studied rotaxanes that consisted of a molecular axle, with a photoactive 9-Aryl-9-methoxy-acridane moiety at one end, and a tetracationic ring of cyclobis(paraquat-p-phenylene) (**CBQT^{4+}**). The aim of the study was to deposit the axle ends onto gold nanoparticles (AuNPs). First, we introduced thioctic acid into the axle molecules. Then, rotaxanes were deposited on AuNPs by two methods: 1) Pseudorotaxanes were deposited on the gold surface by forming rotaxanes with the AuNP as a terminator to prevent unthreading of the ring structure; and 2) a chain containing the thioctic ester was introduced into a complete rotaxane, and then it was deposited on the AuNP with the aid of an exchange process. The photoheterolysis of the acridane unit resulted in formation of the corresponding acridinium methoxide; this, in turn, could thermally react to return to the acridane moiety. Due to the creation of a positive charge, the ring moved from the acridane station to a second, evasive station within the axle. This switching cycle could also take place when deposited on the gold surface. However, on the gold surface, the ring movement associated with the switching process was unidirectional.

1. Introduction

Rotaxanes are supramolecules composed of a threadlike molecule (axle) that incorporates recognition stations and a ring; these two components are mechanically interlocked. Bistable rotaxanes have at least two recognition stations; they are molecular shuttles in which the ring position may be altered. Energy for the shuttling process stems from Brownian motion.[1] Provided that the two stations have sufficiently different interaction strengths with the ring, the ring will reside preferably on one of the two recognition stations. When an outer stimulus weakens the strong interaction of the station on which the ring resides, the ring will move to the station with the originally weaker interaction. Thus, a complete rearrangement of the mechanically bonded components will occur, *i.e.*, a co-conformation,[2] and the shuttle process is referred to as a switch.[1]

Solvent,[3] chemicals,[4] electrons,[5] or light can all serve as stimuli for the switching process. The advantage of light driven systems is that no chemical fuels are necessary and no waste products are formed. The reset can be accomplished either photochemically or thermally.[6]

Control over the relative position and motion of components in interpenetrated molecules, like rotaxane supramolecules, may impart machine-like properties. We have previously reported that photoswitchable rotaxanes have a switching unit of 9-methoxy-9-aryl-acridane and a ring component of cyclobis(paraquat-*p*-phenylene) (**CBQT^{4+}**). Their behaviours in solution have been studied previously.[7] The switching principle consists of the photoheterolysis of the acridanes that form the 9-arylacridinium methoxides. The thermal attack of the methoxide ion on the acridinium ion rebuilds the acridane, thus completing the switching cycle. 9-Arylacridanes are photoresponsive molecular switches that change their geometry, redox potential, and colour upon formation of the corresponding acridinium moiety. The acridinium compounds are metastable and can exist only as long as light is provided. The lifetime of the rotaxanes in their "acridinium state" depends strongly on the composition of the solvent.[7] However, to realise the full potential of these rotaxanes, a triggered motion is required at the transducing surfaces that makes them behave coherently relative to the surface.

Herein, we describe the photochemical behaviour of rotaxanes deposited on gold nanoparticles (AuNPs). Metal NPs have stimulated increasing interest in the past decade.[8] Several switchable molecules deposited on NPs have previously been studied with UV-Vis-spectroscopy and electrochemical methods.[9] However, to the best of our knowledge, photoswitchable, interlocked molecules, like rotaxanes, deposited on AuNPs have not been previously described.

2. Results and Discussion

The immobilisation of photoswitchable rotaxanes on AuNPs is associated with at least two problems: (1) A functional group containing sulfur has to be introduced into the rotaxane in order to use the thiophilicity of gold for attachment; moreover, the functional group should not interfere with the shuttle movement of the rotaxanes. (2) Because the gold surface is able to quench

Institute of Chemistry, Humboldt-Universität zu Berlin, Brook-Taylor-Str. 2, D-12489, Berlin, Germany. E-mail: abraham@chemie.hu-berlin.de

† Electronic supplementary information (ESI) available: Additional experimental information, UV-vis and NMR spectra of selected compounds and transients; assignment of protons of rotaxanes. See DOI: 10.1039/c1ob05128h

photoexcited states,[8,10] the photoreactivity of the photoswitch bound to the gold has to be protected in order to produce a reaction similar to that of the same molecules in solution. A spacer unit between the gold surface and the photoswitch of the rotaxane would be advantageous.

2.1 Syntheses

The molecular threads **2** and **4**, both containing a thioctic ester unit, were synthesised, starting from the previously reported threads **1** and **3**[7] (Scheme 1). The acridinium compounds **2** and **4** were easily transformed into the photoactive acridane compounds **5** and **6**, which can form pseudorotaxanes with the tetracationic ring, **CBQT**$^{4+}$.

A rotaxane with a thioctic acid as an anchor group was synthesised, starting with the protected N-alkyl acridinone **7** (Scheme 2). The pseudorotaxane formed with molecular thread **10** and **CBQT**$^{4+}$ was reacted with adamantoyl chloride to give rotaxane **11** after purification (Scheme 3). Again, the photoactive rotaxane was available by reaction of the acridinium rotaxane with methanol.

Despite the exclusion of air with an argon atmosphere during the preparation, the disulfide bridge was partly oxidised. Nevertheless, the anchor group was able to function (see below).

2.2 Co-conformation of rotaxanes 12 and 13

Apart from the substituent at the N-atom of the acridinium and acridane moieties, rotaxanes **12** and **13**, respectively, were identical to the rotaxanes that bore a methyl group at the same position, which were previously characterised.[7]

The chemically-induced shifts of specific proton signals, both on the ring and on the axle, that were manifest in the ^{1}H-NMR spectra indicated the strength of the interactions between specific regions of the axle with the ring compound. The NMR data of **12** were fully consistent with a rotaxane co-conformation, in which the ring surrounded station B. The proton resonances of the acridinium unit were not shifted with respect to those of the axle in compound **9**. In contrast, the interactions between the ring and station B were accompanied by significant upfield shifts of the aromatic proton resonances and the adjacent protons of the polyether chain; this was caused by strong diamagnetic shielding due to the π-stacking of the bipyridinium ring and station B aromatic systems (Scheme 3 and S3, ESI†).

In contrast to rotaxane **12**, the proton signals in the ^{1}H NMR spectra of **CBQT**$^{4+}$ and of the aryl protons of stations A and B on rotaxane **13** were broad or even merged with the baseline at room temperature (Fig. S1 and S2†). However, the proton signals of the propoxy chain of station B were quite sharp, and therefore, they could be assigned. These proton resonances were low-field shifted compared to those of rotaxane **12**, and they were identical to the proton resonances of compound **10**.

On the other hand, the protons of the acridane subunit and the methoxy group were low-field shifted due to their location at the edge of the ring. Both findings, taken together, clearly demonstrated the occupancy of station A by the ring. ^{1}H NMR spectra recorded at lower temperatures revealed that the tetracationic cyclophane encircled station A. At 233°K, signals were much sharper; the aryl protons of the two stations were apparent and could be assigned by C–H-, H–H-COSY, and ROESY spectra. The protons of station A were upfield shifted by 2.5 and 3.9 ppm (Fig. S2b†). Due to the asymmetry of the axle, the bipyridinium protons appeared as four broad singlets, and the protons of the methylene groups of **CBQT**$^{4+}$ were split into two doublets of the AB-system (Scheme S4†).

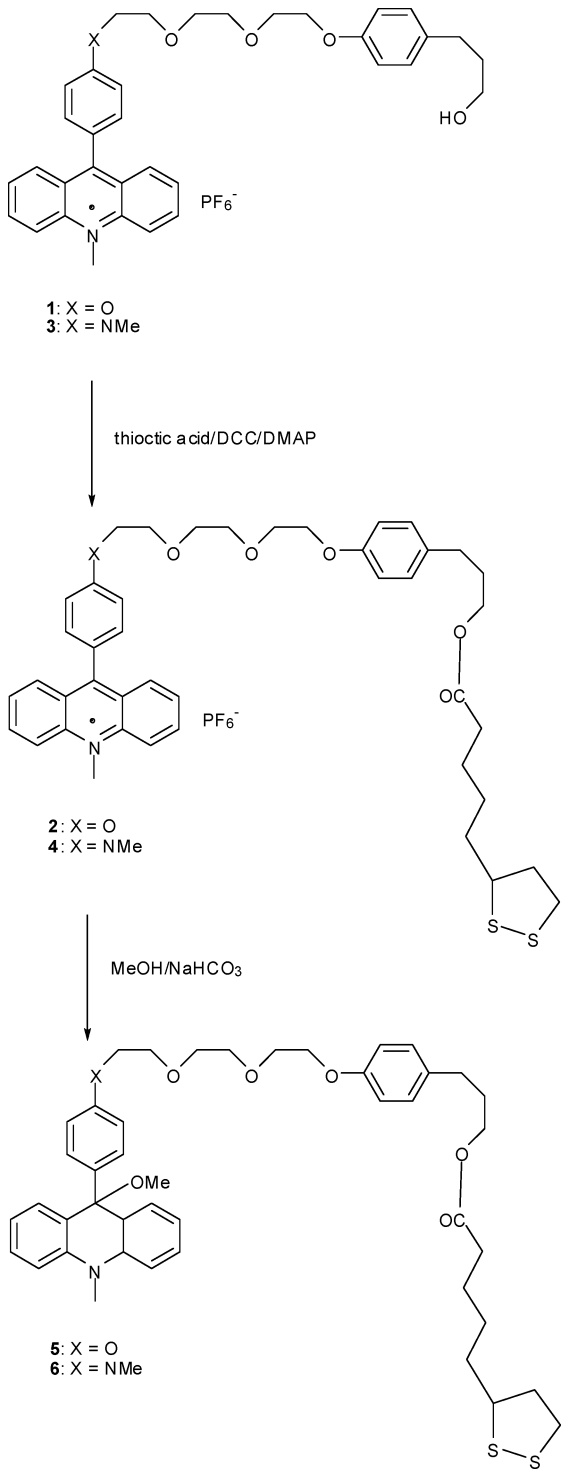

Scheme 1 Synthesis of axles containing thioctic ester.

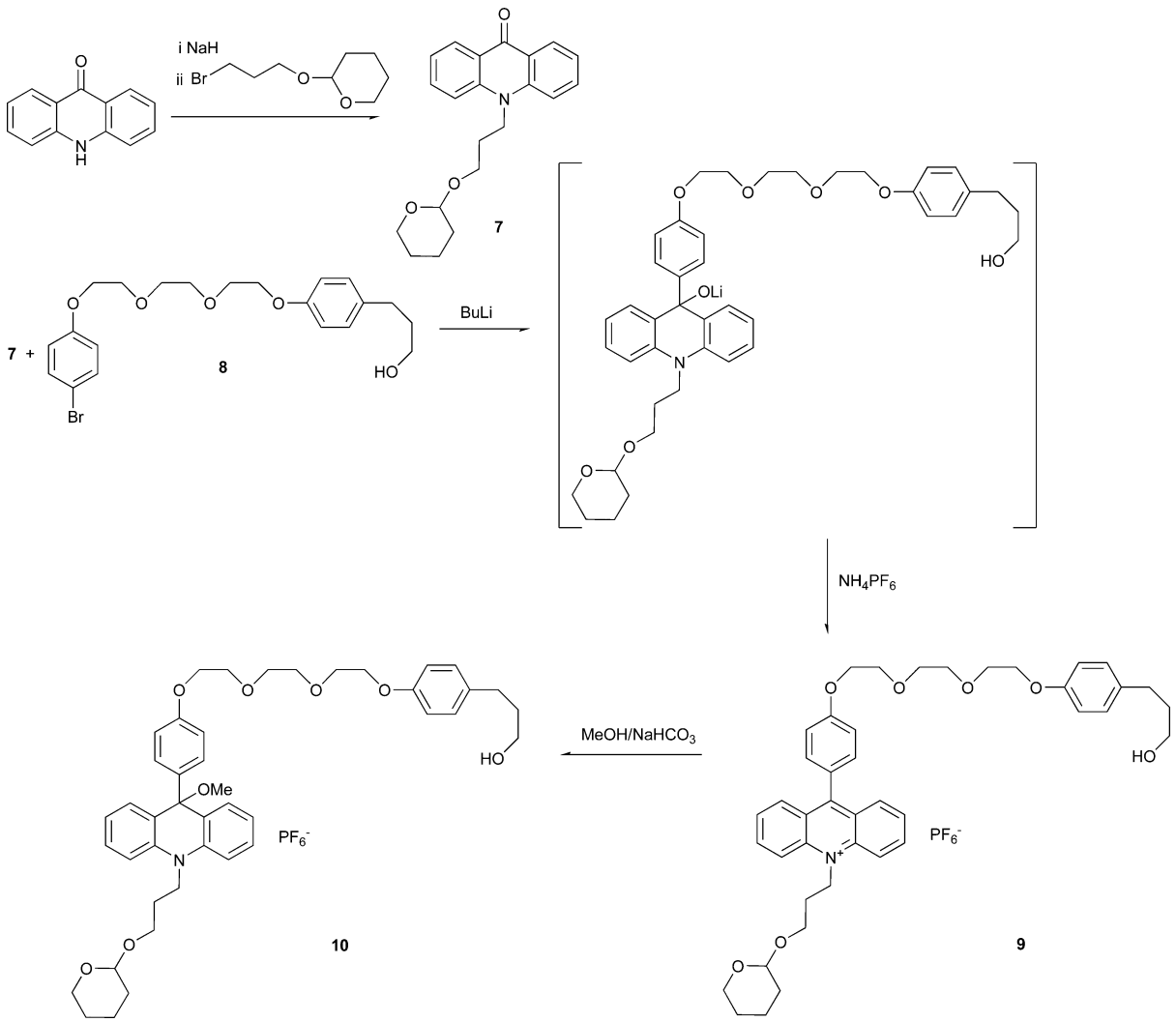

Scheme 2 Synthesis of protected axles.

2.3 Synthesis of capped AuNPs

The AuNPs coated with **2**, **4–6**, **12**, and **13** were synthesised by ligand-exchange reactions.[11] To maintain stable dispersion of the AuNPs, we employed dodecane thiol as a stabilising agent.[12]

Solutions of thiol-capped AuNPs in dichloromethane were mixed with acetonitrile solutions of compounds **2**, and **4–6**, without and with **CBQT**$^{4+}$ and **13**, respectively. After stirring for 3 days under an argon atmosphere, the solvents were evaporated. To remove unbound compounds, the residue was washed with acetonitrile until no UV/Vis-absorption of the wash solutions could be detected. The average sizes of the AuNPs were between 2.8 and 3.4 nm (Fig. S3–S6†). According to the average diameter and the elemental analysis, AuNPs were decorated with four thiol molecules (ESI†). Only one molecule of rotaxane **13** was deposited on the AuNPs.

2.4 Photochemistry of immobilised molecular threads

To explore the photoheterolysis of acridanes on gold surfaces, compounds **5** and **6** were deposited on AuNPs and irradiated with >300 nm light in dichloromethane (DCM)/methanol (8 : 2) solution. The UV-Vis absorption spectrum corresponded to that of the free compounds recorded in the same solvent mixture (Fig. 1). The smoothly increasing baseline was caused by the absorption of the AuNPs (surface plasmon resonance). The photoreaction was easy to follow with UV-Vis spectroscopy, because only the corresponding acridinium compounds formed by photoheterolysis were able to absorb light above 350 nm (Fig. 1). Isosbestic points revealed that the photoreactions of the acridanes on AuNPs were the same as those of the free compound in solution.

The efficiencies of the photoreactions of **5** and **6** deposited on AuNPs were comparable to that of the photoreactions of the free compounds. Clearly, the photoexcited state of the acridanes was not quenched by the gold surface. When comparable concentrations of free **5** and **5** bound to AuNP were irradiated for 5 s with > 300 nm light, we observed comparable initial increases of absorbance at 360 nm (acridinium compound; Fig. 2). However, the irreversible formation of acridinium compounds was much higher when **5** was deposited on AuNPs than when **5** was in solution. This was shown by the decay of the transient absorbance after irradiation at 360 nm; the residual absorbance of **5** on AuNP

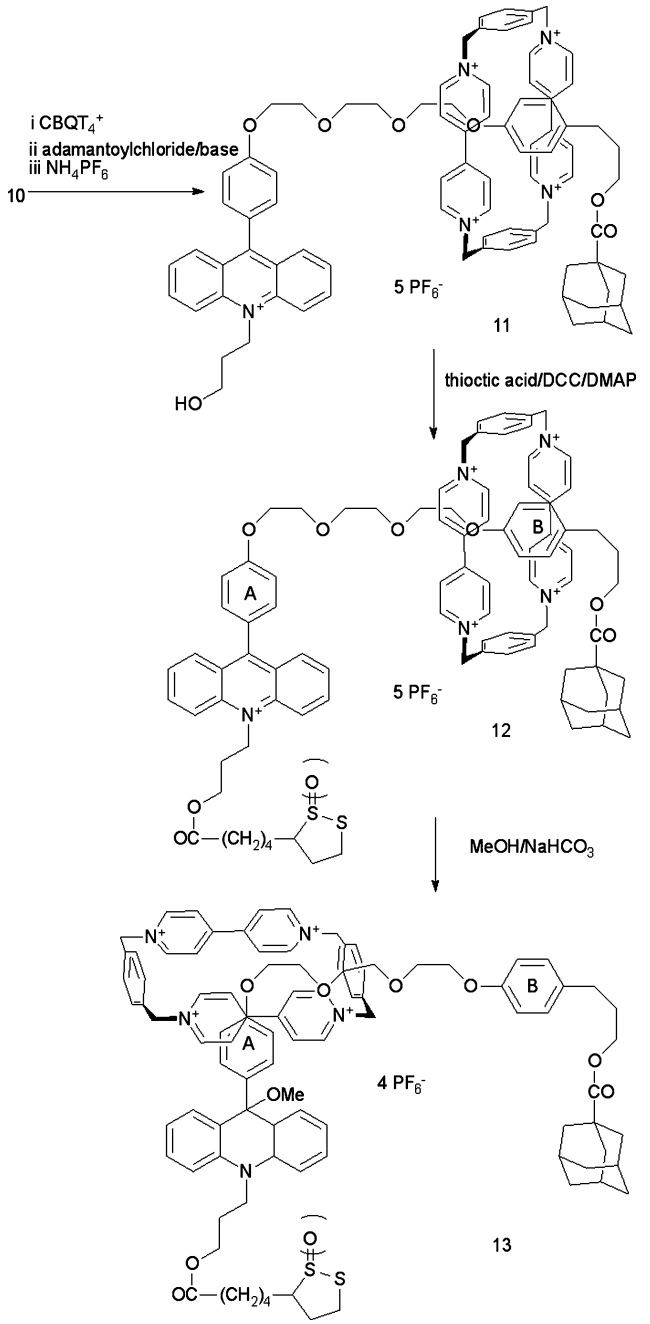

Scheme 3 Synthesis of rotaxanes containing thioctic ester within the axle.

was higher than that of free **5** in solution (compare the curves in Fig. 2). This indicated that the methoxide ions released upon photolysis of the acridane compound did not completely react with acridinium ions at the AuNP surface.

The transient UV-Vis absorption spectra was visualised by subtraction of the spectra recorded before from the spectra recorded after the irradiation. This clearly showed the formation of the acridinium methoxides (*e.g.*, compound **6** in Fig. 3).

The lifetime of the transient acridinium methoxide formed on AuNPs upon irradiation was considerably shorter than that of the acridinium methoxide formed in solution (compare Fig. 3b and 3c). Consequently, these results showed that the photoheterolysis of acridanes could take place on gold surfaces, but with

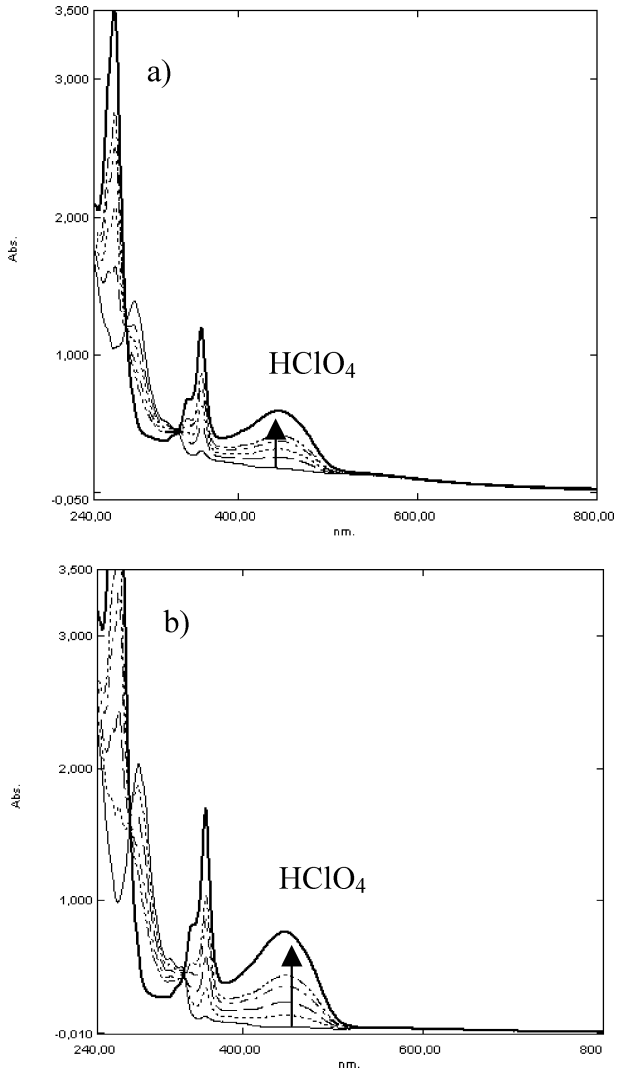

Fig. 1 a) Spectra of AuNP/**5** recorded after irradiation (5, 10, 15, 20, 25 s) with light of wavelengths > 300 nm in DCM/MeOH (8 : 2) solution. Black curve: addition of $HClO_4$; b) Spectra of **5** in DCM/MeOH recorded after irradiation (0, 5, 10, 15, 20 s). Black curve: addition of $HClO_4$.

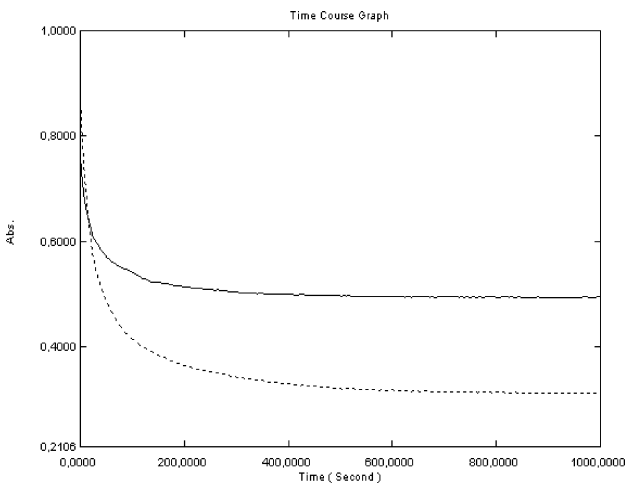

Fig. 2 Decay curves of the absorbance at 360 nm recorded after a 5 s irradiation in DCM/MeOH (4 : 1). Continuous line: **5** on AuNP; dotted line: free **5** in solution.

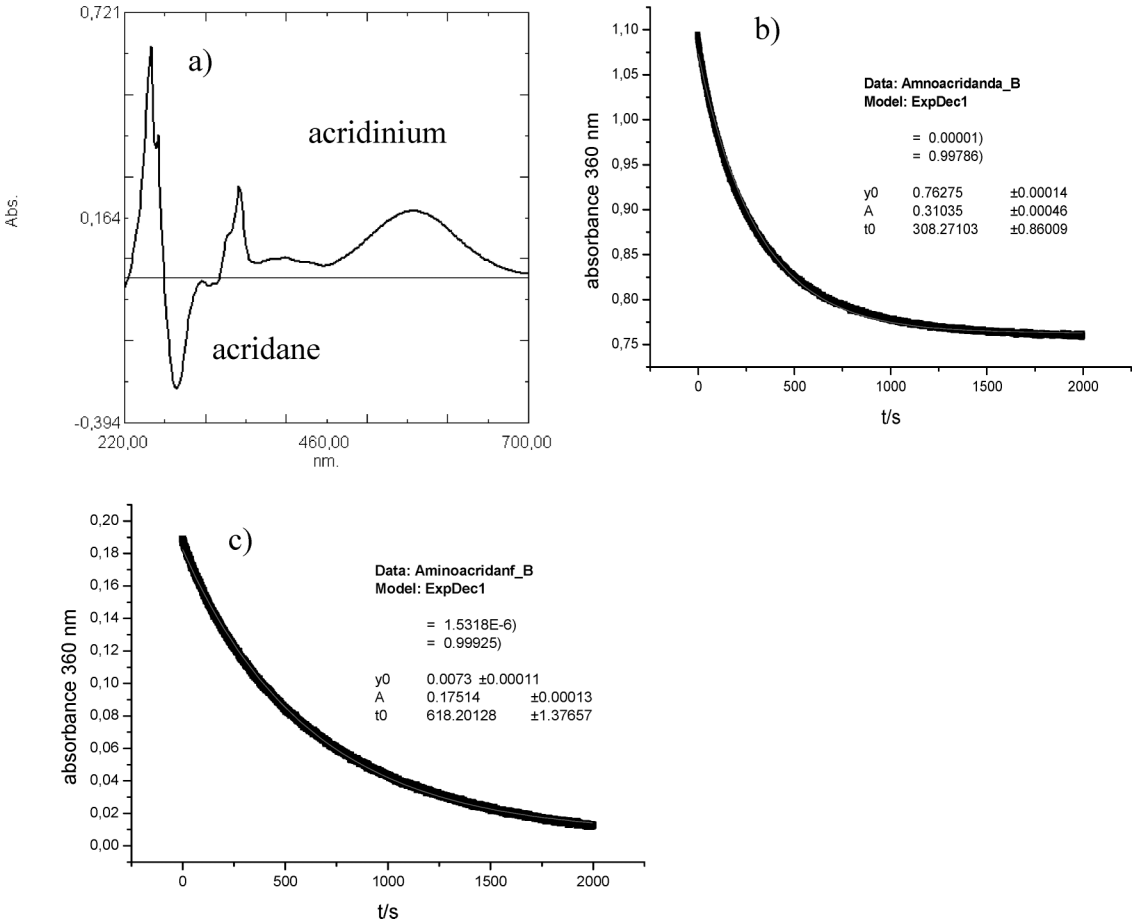

Fig. 3 Transient absorption spectra recorded after irradiation. (a) Transient absorption after 5 s irradiation at >300 nm of compound **6** deposited on AuNP in DCM/MeOH/MeCN (1 : 10 : 10) solution; (b) decay curve of the transient absorbance of **6** on AuNP at 360 nm; (c) decay curve of the transient absorbance of **6** in DCM/MeOH/MeCN (1 : 10 : 10) solution.

diminished recovery of the acridane compared to photoheterolysis of free acridanes in solution (Scheme 4).

2.5 Rotaxanes on AuNP

2.5.1 Pseudorotaxanes on AuNP.

*2.5.1.1 Interactions with **CBQT**$^{4+}$.* We expected that, when the exchange of dodecanethiol by threads **5** and **6** was carried out in the presence of **CBQT**$^{4+}$, it would induce the formation of rotaxanes on the AuNP surface; in this reaction, the AuNP would act as one of the two necessary terminators that could prevent dethreading of the ring (Scheme 5).

In fact, NMR spectra of the capped AuNPs in $CDCl_3/CD_3CN$ solution exhibited both the proton signals of threads **5** or **6** and those of **CBQT**$^{4+}$ in a 1 : 1 ratio (Scheme S1, ESI†).

As expected, the acridinium compounds were not able to bind **CBQT**$^{4+}$ on the AuNPs.

Typical of acridane rotaxanes, in the ^{1}H NMR spectra, the proton signals of **CBQT**$^{4+}$ and the aryl protons of rotaxanes were broad or even merged with the baseline at room temperature.[7] However, the proton signals of the propoxy chain of the aryl station B (Scheme 5) were relatively sharp, and therefore, they could be assigned (Schemes S1 and S2). These proton resonances were identical with those of the same protons in compounds **5** and **6**. These findings indicated that the ring **CBQT**$^{4+}$ resided on the acridane station A. Surprisingly, the proton signals of **CBQT**$^{4+}$ were not shifted by complexation with the axle on the gold surface.

2.5.1.2 Photoreaction of pseudorotaxanes on AuNPs. The rotaxanes formed between **CBQT**$^{4+}$ and **5** and **6** on the AuNP surface were photoactive. Upon irradiation with >300 nm light, the acridane station A was converted to the acridinium moiety. The transient UV-Vis absorption of the photoproduct clearly showed the formation of the acridinium rotaxane (Fig. 4 and S7, ESI†). Accordingly, the ring moved from the newly-formed acridinium station towards station B. The thermal reaction between the methoxide and the acridinium ion restored the starting co-conformation.

In comparing Fig. 2 and 4, it is clear that the efficiency of the photoreaction was strongly diminished in the latter. A much smaller increase of the transient absorption was observed with comparable excitation conditions, including the absorbance at the irradiation wavelength and the light intensity (Fig. S7†). The reaction with the pseudorotaxane **6**/**CBQT**$^{4+}$ on AuNP showed lower efficiency than with **5**/**CBQT**$^{4+}$. The lower efficiencies of the pseudorotaxanes on AuNP compared to free **5** and **6** could be attributed to the charge-transfer interaction between the acridane station A and **CBQT**$^{4+}$ and the filter effect of the UV-absorption

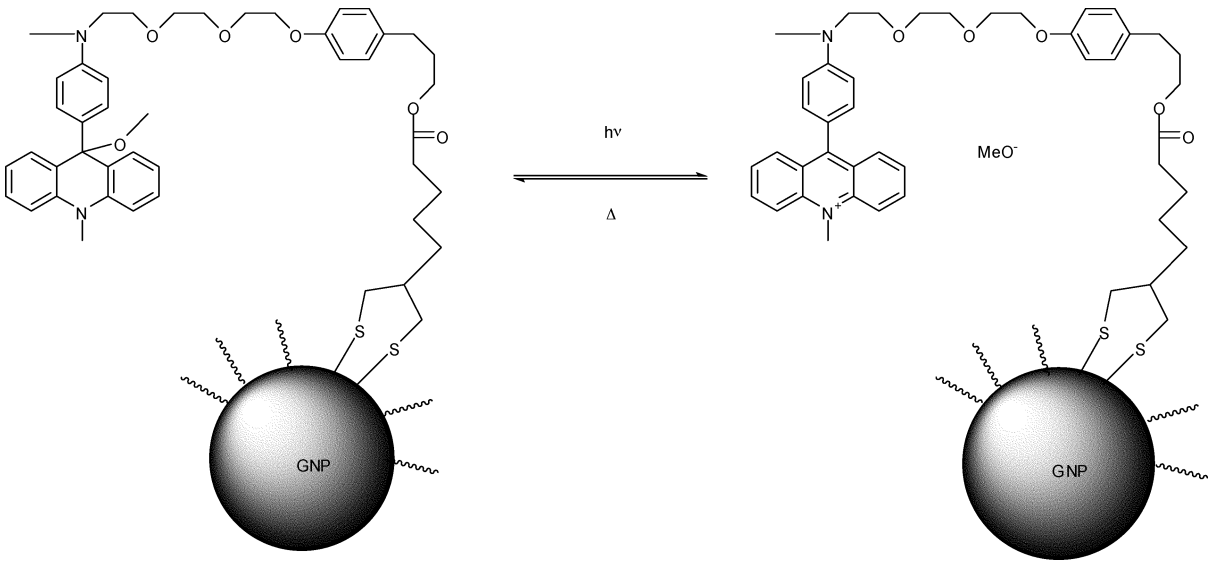

Scheme 4 Switching cycle on AuNP.

of the ring. The same finding was observed in solution with comparable rotaxanes.[7]

2.5.2 Rotaxanes 12 and 13.

2.5.2.1 Ring movements. In accordance with the results obtained for rotaxanes in solution, **CBQT**$^{4+}$ resided on station B of rotaxane **12**. In contrast, the acridane station A was predominantly occupied in rotaxane **13**. The strong upfield shifts of proton signals of station B in **12** and of station A in **13** revealed the position of the ring on the axle (Scheme S5 and S6; Fig. S8, S9†).

Because the acridinium moiety was formed by the photolysis of the acridane station, the ring moved from station A to station B. The attack of the methoxide ion on the acridinium unit reconverted the acridane station, thus starting a new ring movement.[7]

*2.5.2.2 Photoheterolysis of **13** in solution.* The transient UV-Vis-absorption spectra observed upon irradiation of rotaxane **13** in solution (DCM/MeOH/MeCN 1 : 10 : 10 and ethanol) indicated the presence of two species. The disappearance of the acridane chromophore (negative absorption at 285 nm) was accompanied by increased absorbances at 260, 360, and 430 nm, which was the characteristic absorption spectrum of the acridinium chromophore. However, the absorption peaks at 410 and 620 nm were attributed to the radical trication, **CBQT**$^{\bullet 3+}$, generated by photoinduced electron transfer from the acridane moiety to the tetracationic ring.[12,13] Accordingly, the radical trication of **CBQT**$^{4+}$ was not formed upon irradiation of **12**.

The radical cation of the acridane moiety decomposed to the acridinium ion and the methoxy radical. The latter took up an electron from **CBQT**$^{\bullet 3+}$; this resulted in the same products as those formed by a direct photolysis of the acridane moiety.[12]

It is noteworthy that the electron transfer was more effective in ethanol solution (compare Fig. 5a and 5b). The lifetime of the absorbance at 360 nm, which was assigned to the acridinium methoxide, was 1400 s in the solvent mixture and 840 s in ethanol. In contrast, the decay of **CBQT**$^{\bullet 3+}$ monitored at 620 nm was faster (lifetime 200 s in ethanol solution; Fig. S10, ESI†).

This switch cycle could be repeated at least ten times. However, about 2% of the acridinium rotaxane was irreversibly formed in each cycle (Fig. S11†).

*2.5.2.3 Photoheterolysis of **13** on AuNP.* The UV-Vis spectra of AuNPs coated with rotaxane **13** exhibited both the absorbance of the AuNPs and the typical absorption spectrum of the acridane rotaxane. The latter comprised a superposition of the acridane chromophore (320 and 280 nm) and the ring, **CBQT**$^{4+}$ (260 nm). Upon addition of diluted acid, the absorption spectrum of the acridinium rotaxane **12** appeared (Fig. 6).

The rotaxane **13** deposited on AuNPs was irradiated in a solvent mixture of DCM/MeCN/MeOH (1 : 10 : 10) with light of wavelengths > 300 nm. Transient UV-Vis spectra clearly indicated the formation of the corresponding acridinium rotaxane (Fig. 7). The absorbance at 260, 360, and 430 nm was attributed to the acridinium chromophore of rotaxane **12**. The negative absorbance at 283 nm corresponded to the disappearance of the acridane chromophore of **13**. Absorption bands at 410 and 620 nm were attributed to the radical trication, **CBQT**$^{\bullet 3+}$. The appearance of the radical trication spectrum indicated that electron transfer from the acridane moiety to **CBQT**$^{4+}$ also played a role in depositing rotaxane **13**, as it was observed in solution. However, the fraction of radical trications was significantly higher with AuNPs than in solution (compare Fig. 5a and 7).

The productive electron transfer from the acridane moiety to the tetracationic ring could again transform the acridane unit into the acridinium unit. Accordingly, after the dark reaction, the initial absorbance of rotaxane **13** was restored. The cycle of photoreaction – thermal back reaction could be repeated several times without significant fading of the acridane absorbance.

The decay of the absorbance at 360 nm corresponded to the lifetime of the acridinium rotaxane with methoxide as counterion (Fig. S12, ESI†). This 60 s decay was considerably shorter than that measured in solution (60 *vs.* 1400 s, see above).

Converting the acridane rotaxane into the acridinium rotaxane was accompanied by the movement of the ring **CBQT**$^{4+}$ from the acridane station to the evasive station B (Scheme 6). Accordingly,

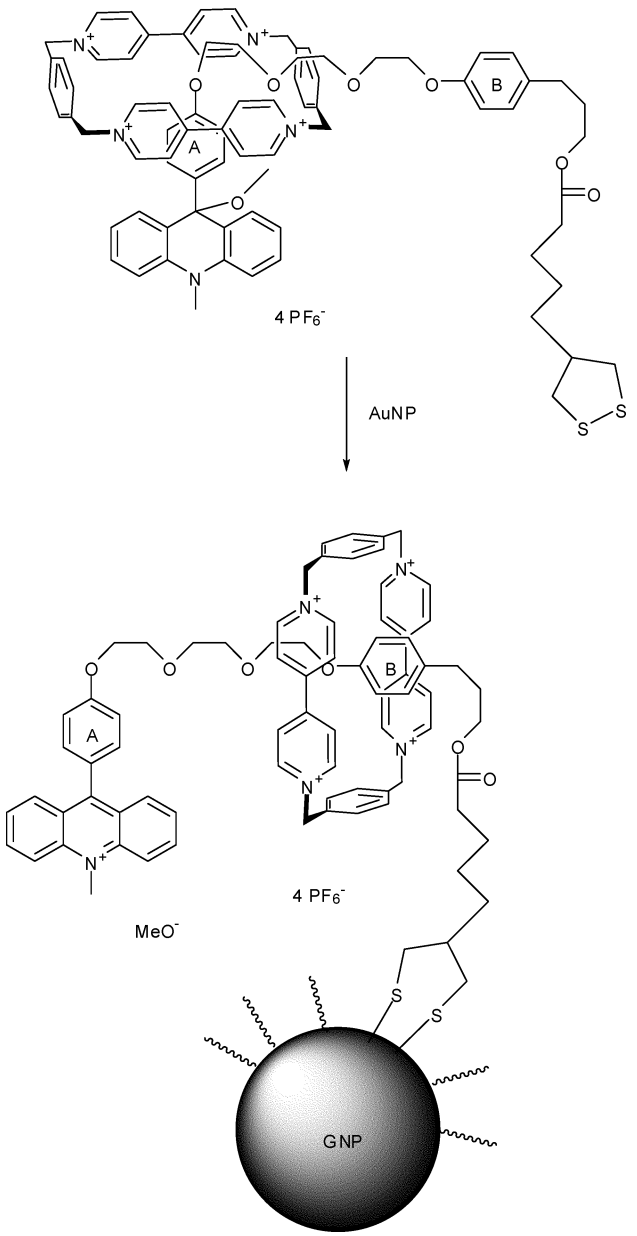

Scheme 5 Deposition of a pseudorotaxane on AuNP.

in the acridinium state, the ring was more distant from the surface. With respect to the surface of the AuNP, the movement was unidirectional.

3. Conclusions

We have shown that thiol-protected gold nanoparticles could successfully be functionalised with 1) photoactive molecular threads that contained both the acridane unit and an evasive station, 2) pseudorotaxanes formed between these threads and the **CBQT**$^{4+}$ wheel, and 3) bistable [2]rotaxane molecules that contained both the acridane unit and the evasive station. Both of these molecular threads, the pseudorotaxane and the rotaxane retained photoreactivity and switching properties at the nanoparticle-solvent interface.

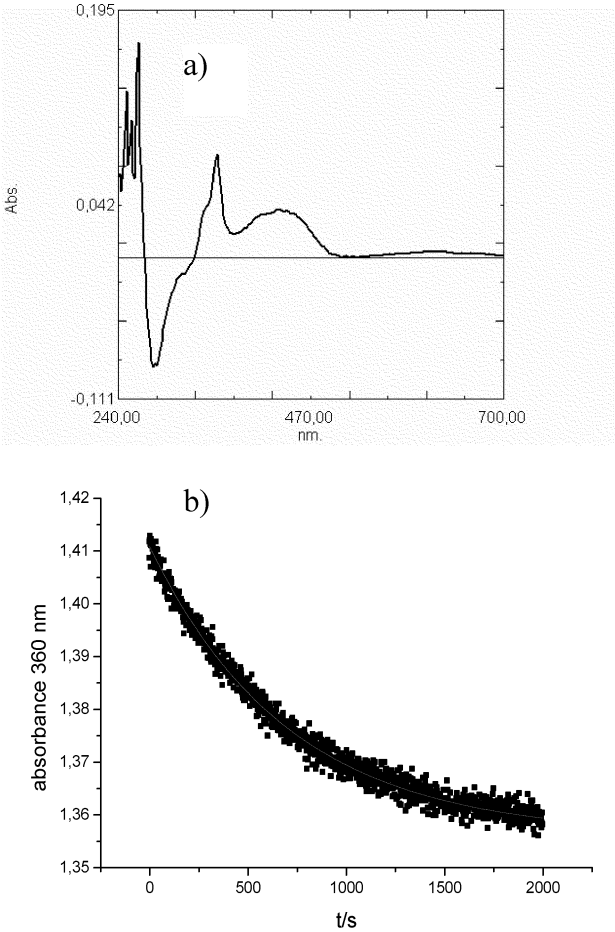

Fig. 4 a) Formation of the acridinium rotaxane. Transient absorption spectrum recorded after irradiation (<300 n m) of pseudorotaxane **5/CBQT**$^{4+}$ immobilised on AuNP in DCM/MeOH/MeCN (1 : 10 : 10 solution); b) decay curve of the transient absorbance at 360 nm.

Acridinium methoxides were formed from the corresponding acridane molecules, both by direct photoheterolysis and by photoinduced electron transfer from the acridane moiety to the **CBQT**$^{4+}$. Switch cycles could be repeated several times without precipitation of the dispersed nanoparticles. In the switch cycle, the ring **CBQT**$^{4+}$ moved between the acridane station near the surface and the evasive station more distant from the surface. Related to the AuNP surface, the movement was unidirectional.

4. Experimental

General methods

Commercially available chemicals and solvents (UVASOL, Merck) were used as received, unless otherwise noted; solvents were dried according to standard procedures. Column chromatography (CC) was carried out on 200 mesh silica gel (Merck). Melting points were determined with a Boetius heating microscope.

Electrospray ionisation mass spectroscopy was carried out on a LTQ-FT (Finnigan MAT, Bremen, Germany), equipped with an electrospray ion source (Thermo Electron).

NMR spectra were recorded on a Bruker DPX 300 (300 MHz) and a Bruker Advance 400 (400 MHz). The proton signals were attributed to the different subunits with the aid of

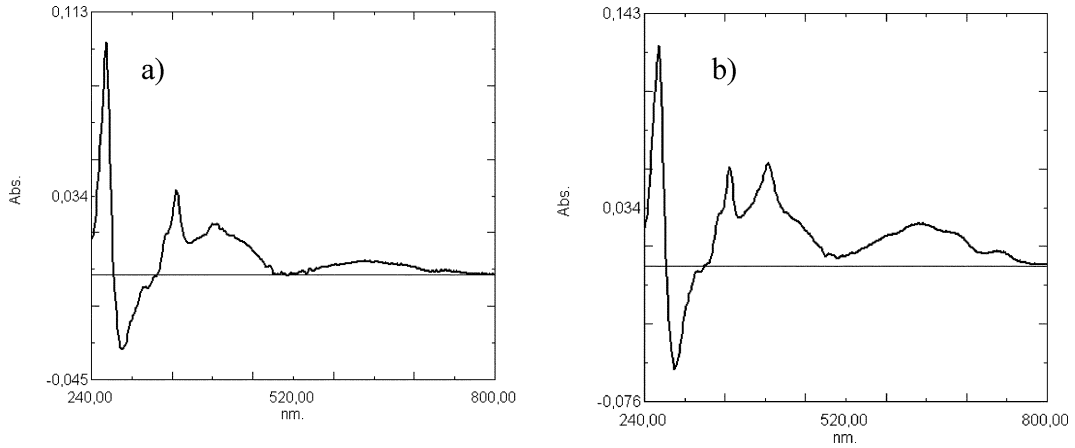

Fig. 5 Transient absorption spectrum monitored after irradiation of **13** (5 s HBO 500; >300 nm). a) in a solvent of DCM/MeCN/MeOH (1 : 10 : 10); b) in a solvent of ethanol.

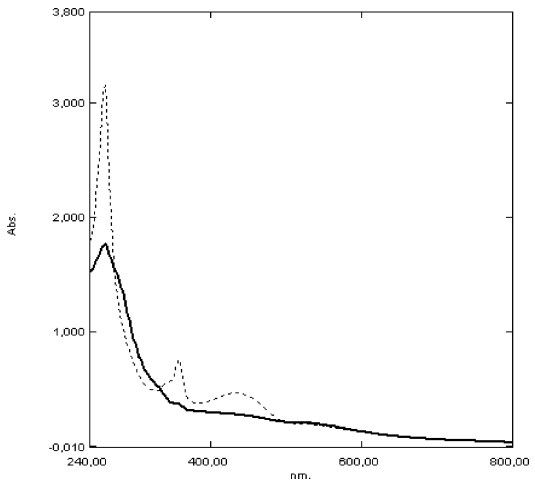

Fig. 6 UV-Vis spectrum of rotaxane **13** on AuNP in DCM/MeCN/MeOH (1 : 10 : 10) solution. Continuous line: UV-Vis spectrum of rotaxane **13** on AuNP in solution; Dotted line: UV-Vis spectrum of rotaxane **12** generated from **13** by the addition of $HClO_4$.

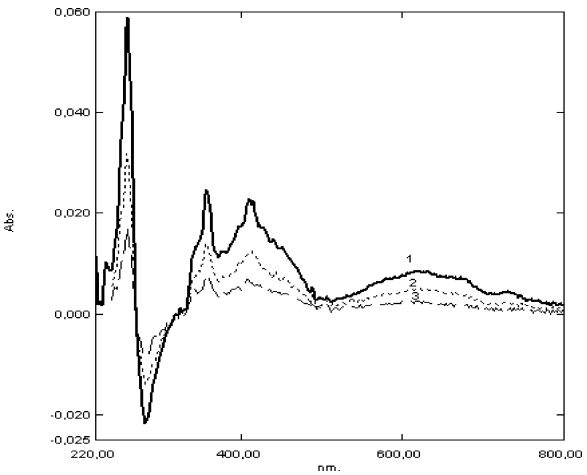

Fig. 7 Transient absorption spectra recorded after irradiation of **13** (5 s) deposited on AuNP in DCM/MeCN/MeOH (1 : 10 : 10). (1) recorded immediately after irradiation; (2) recorded after a 3 min delay; (3) recorded after a 10 min delay.

two-dimensional NMR spectroscopy, including C-H-COSY, H-H-COSY, and ROESY.

UV/Vis measurements were performed with a Shimadzu UV 2101 PC spectrometer.

Irradiations of the rotaxane solutions were carried out with a conventional mercury arc (HBO 500 or HBO 200) combined with a cut-off filter of 300 nm. Transient absorption spectra between 240 and 500 nm were recorded with the UV 2101 PC spectrometer, using the fastest scan mode. Turnover of acridinium ions generated by photolysis was determined by comparing the absorbance at 360 nm with the absorbance obtained upon addition of HClO4.

Transmission electron microscopy (TEM) experiments were performed using a Tecnai F20 (FEI Company, Oregon, USA) microscope equipped with a field emission gun operating at an accelerating voltage of 160 kV. Images were recorded using an EAGLE 2k-CCD device (FEI Company, Oregon, USA) at full 2048 by 2048 pixel size and a primary magnification of 240k. Specimen preparation for TEM: TEM samples were prepared by depositing a droplet of the suspension (5 µl) onto a carbon covered copper grids (400 mesh) which had been hydrophilized prior to use by a 60 s plasma treatment at 8 W in a BAL-TEC MED 020 device (Leica Microsystems, Wetzlar, Germany). Supernatant fluid was removed after 30 s incubation by blotting with a filter paper until an ultrathin layer of the sample was obtained. The air-dried specimens were transferred into the microscope for imaging.

Syntheses

Assignments of NMR-signals of new compounds are given in the ESI.†

9-(4-(2-(2-(2-(4-(3-(5-(1,2-Dthiolan-3-yl) pentanoyloxyl) propyl) phenoxy) ethoxy)ethoxy)ethoxy)phenyl)-10-methylacridinium hexafluorophosphate (2). **1**[7a] (0.71 g, 1.25 mmol), thioctic acid (0.31 g, 1.5 mmol), N,N′-dicylohexyl-carbodiimide (0.31 g, 1.5 mmol) and 4-dimethylamino-pyridine (0.04 g, 0.25 mmol) were dissolved in dichloromethane (25 mL) and stirred for 3 days under argon. After filtration and removal of solvents, the crude product was purified by column chromatography (silica gel, isopropanol/water/acetic acid = 5 : 2 : 1). The product was dissolved in dichloromethane (10 mL) and mixed with a solution

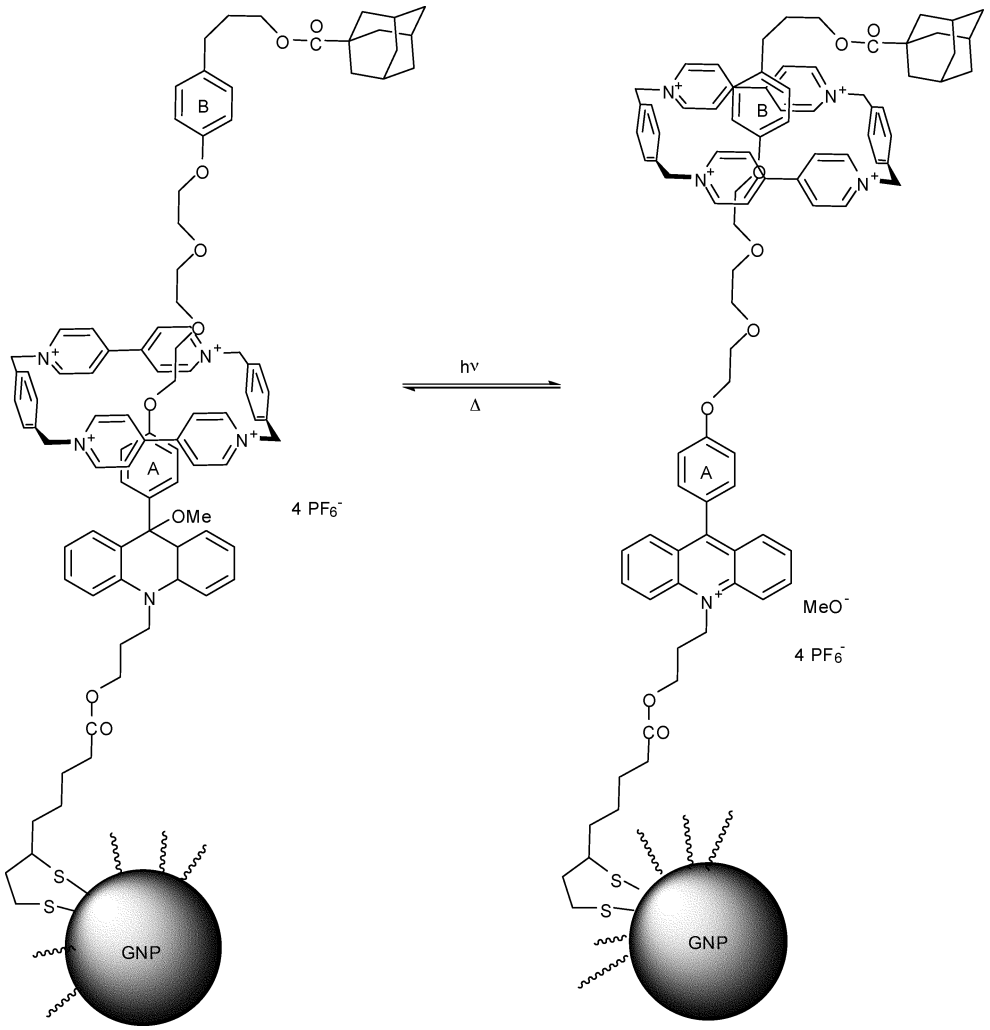

Scheme 6 Switching cycle of rotaxane **13** on AuNP.

of ammonium hexafluorophosphate (0.2 g, 1.25 mmol) in water (50 mL). The aqueous phase was separated and extracted with dichloromethane. The combined extracts were washed with water. The combined organic layers were dried over $MgSO_4$. After filtration and removal of solvents, the residue was dried *in vacuo* to give the product as red solid (0.76 g, 81%), m.p. 195–198 °C. $C_{43}H_{50}F_6NO_6PS_2$ (885.27): calcd. (%): C 54.32, H 5.36, N 1.86, S 8.53; found (%): C 54.29, H 5.38, N 1.84, S 8.45.

HRMS (ESI): *m/z*: found 740.3997; calcd for $[M–PF_6^-]$ $[C_{43}H_{50}NO_6S_2]^+$ 740.3980.

9-(4-(2-(2-(2-(4-(3-(5-(1,2-Dithiolan-3-yl)pentaoyloxy)propyl)-phenoxy) ethoxy)ethoxy)ethyl)methylamino)phenyl)-10-methyl-acridinium hexafluorophosphate (4). **3**[7b] (1.04 g, 1.46 mmol), thioctic acid (0.31 g, 1.5 mmol), N,N′-dicylohexyl-carbodiimide (0.31 g, 1.5 mmol) and 4-dimethylamino-pyridine (0.04 g, 0.25 mmol) were dissolved in dichloromethane (25 mL) and stirred for 3 days under argon. After filtration and removal of solvents, the crude product was purified by column chromatography (silica gel, isopropanol/water/acetic acid 5 : 2 : 1). The product was dissolved in dichloromethane (10 mL) and mixed with a solution of ammonium hexafluorophosphate (0.2 g, 1.25mmo) in water (50 mL). The aqueous phase was separated and extracted with dichloromethane (3 × 10 mL). The combined extracts were washed with water. The organic layer was dried over $MgSO_4$. After filtration and removal of solvents, the residue was dried *in vacuo* to give the product as dark violate solid (1.22 g, 91%), m.p. 175-178 °C. $C_{44}H_{53}F_6N_2O_5PS_2$ (899.00): calcd. (%): C 58.78, H 5.94, N 3.12, S 7.13; found (%): C 58.65, H 5.99, N 3.30, S 7.33; HRMS (ESI): *m/z*: found 753.3380; calcd for $[M–PF_6^-]$ $[C_{44}H_{53}N_2O_5S_2]^+$ 753.3390.

3-(4-(2-(2-(2-(4-Methoxy-10-methyl-4a,9,9a,10-tetrahydro-acdrin-9-yl)phenoxy)ethoxy)ethoxy)ethoxy)phenyl)propyl-5-(1,2-dithiolan-3-yl)pentanoate (5). **2** (100 mg, 0.11 mmol) dissolved in MeCN/MeOH (10 mL/2 mL) and K_2CO_3 (150 mg) were vigorously stirred for 4 h. After filtration and removal of solvents, the crude product was treated with dry chloroform (3 × 5 mL). After filtration the solution was evaporated *in vacuo* to afford the product as colorless oil (0.76 g, 89%). $C_{44}H_{53}NO_7S_2$ (772.03): calcd. (%): C 68.45, H 6.92, N 1.81, S 8.31; found (%): C 68.32, H 6.66, N 1.84, S 8.28.

3-(4-(2-(2-(2-(4-Methoxy-10-methyl-9,10-dihydroacdrin-9-yl)-phenyl) methylamino)ethoxy)ethoxy)ethoxy)phenyl)propyl-5-(1,2-dithiolan-3-yl)pentanoate (6). **4** (300 mg, 0.382 mmol) dissolved

in MeCN/MeOH (10 mL/2 mL) and K_2CO_3 (150 mg) were vigorously stirred for 4 h. After filtration and removal of solvents, the crude product was dissolved in dry chloroform (20 mL). After filtration the solvent was evaporated *in vacuo* to afford the product as dark oil (235 mg, 78%). $C_{45}H_{56}N_2O_6S_2$ (785.07): calcd. (%): C 68.85, H 7.19, N 3.57, S 8.17; found (%): C 68.62, H 7.34, N 3.36, S 8.36; HRMS (ESI): *m/z*: found 823.3220; calcd for $[M+K]^+$ $[C_{45}H_{56}KN_2O_6S_2]^+$ 823.3211.

10-(3-(tetrahydro-2*H*-pyran-2yloxy)propyl)acridin-9(10H)-one (7). Acridin-9(10H)-one (0.98 g, 5 mmol) was suspended in anhydrous DMF (20 mL). NaH (0.223 g, 5.6 mmol, 60% in oil) was added and the the mixture was stirred for 6 h under argon at room temperature. 2-(3-bromopropoxy)tetrahydro-2*H*-pyran (2.24g,10 mmol) was added and the reaction mixture was stirred for 20 h at 60 °C under argon. After cooling down to room temperature, the reaction mixture was poured into water (20 ml). The aqueous layer was extracted with diethyl ether (3 × 100 mL). The combined organic phases were washed with water (100 mL), Brine (50 mL) and water (50 mL). The organic layers were dried over $MgSO_4$. The solvent was removed, the residue was extracted with petroleum (25 ml) for 1h. After filtration, the precipitate was dried *in vacuo* to give the product as light yellow powder (1.08 g, 64%), m.p. 138–142 °C.; $C_{21}H_{23}NO_3$ (337.41): calcd. (%): C 74.75, H 6.87, N 4.15; found (%): C 74.55, H 6.95, N 4.04; HRMS (ESI): *m/z*: found 339.1729; calcd for $[M+H^+]^+$ $[C_{21}H_{24}NO_3]^+$ 338.1751.

9-(4-(2-(2-(2-(4-(3-Hydroxypropyl))phenoxy)ethoxy)ethoxy)-ethoxy)phenl)-10-(3-(tetrahydro-2*H*-pyran-2-yloxy)propyl)acridinium hexafluorophosphate (9). 8[7a] (1.69 g, 3.85 mmol) was dissolved in dry THF (55 mL) and cooled down to −78 °C. BuLi (4.8 mL, 5.92 mmol (1.6 M in hexane) was added dropwise within 30 min to this solution at −78 °C under argon. **7** (1.3 g, 3.85 mmol) in dry THF (25 mL) was added dropwise to the reaction mixture within 90 min at −78 °C under argon. The reaction mixture was warmed up to room temperature and stirred over night. Water (2 mL) was poured into the reaction mixture. After filtration and removal of solvents, the residue was purified by column chromatography (silica gel, acetonitrile: 5% aqueous solution of NH_4PF_6 40 : 1). The yellow fractions were collected. The solvents were removed *in vacuo*. The residue was extracted with dichloromethane (50 mL). The filtrate was washed with water (2 × 10 mL). The organic phase was dried ($MgSO_4$). The solvent was evaporated to give the product as yellow, viscous oil (1.21 g, 38%). $C_{42}H_{50}F_6NO_7P$ (825.81): calcd. (%): C 61.09, H 6.10, N 1.70; found (%): C 60.80, H 6.45, N 1.56; HRMS (ESI): *m/z*: found 680.3648; calcd for $[M-PF_6^-]^+$ $[C_{42}H_{50}NO_7]^+$ 680.3582.

3-(4-(2-(2-(2-(4-(9-Methoxy-10-(3-(tetrahydro-2*H*-pyran-2yloxy)propyl)-9,10-dihydroacridin-9-yl)phenoxy)ethoxy)ethoxy)-ethoxy)phenyl)propan-1-ol (10). 9 (0.60 g, 0.73 mmol) dissolved in MeCN/MeOH (25 mL/10 mL) and K_2CO_3 (0.5 g) were vigorously stirred for 24 h. After filtration and removal of solvents, the crude product was uptaken with dry chloroform (30 mL). The suspension was filtered and the filtrate was evaporated *in vacuo* to give the product as oil (0.458 g, 88%). HRMS (ESI): *m/z*: found 750.3409; calcd for $[M+K]^+$ $[C_{43}H_{53}KNO_8]^+$ 750.3403.

Rotaxane 11. 10 (0.443 g, 0.62 mmol), $CBQT(PF_6)_4$ (0.823 g, 0.75 mmol) and 2,6-di(*ter*)butyl-4-methyl-pyridin (0.14 g, 0.69 mmol) were dissolved in acetonitrile (8 mL) and stirred under argon for 1 h at room temperature. A solution 1-adamantoyl chloride (0.124 g, 0.62 mmol) in acetonitrile (2 mL) was added dropwise within 45 min. The reaction mixture was stirred under argon for 5 days. After filtration and removal of solvents the residue was washed with dichloromethane until the solution was colorless. The precipitate was washed with 2 mL of a mixture of MeCN (400 mL), NH_4PF_6 (7 g), ethyl acetate (200 mL) and cyclohexane (100 mL). After filtration the filtrate were purified by the help of column chromatograohy (silica gel, acetonitrile (400 mL), NH_4PF_6 (7 g), ethyl acetate (200 mL), cyclohexane (100 mL). The collected yellow fractions were evaporated. The residue was treated with water (20 mL) and dried *in vacuo* to give the product as yellow powder (0.341 g, 27%), m.p. 218–222 °C. $C_{84}H_{88}F_{30}N_5O_7P_5$ (2003.49): calcd. (%): C 50.33, H 4.33, N 3.49; found (%): C 50.12, H 4.53, N 3.26.

Acridinium Rotaxane 12. 11 (0.150 g, 0.075 mmol) was dissolved in MeCN (1 mL) and mixed with a dichloromethane (12 mL) solution of thioctic acid (0.017 g, 0.082 mmol), N,N′- dicylohexyl-carbodiimide (0.017 g,0.082 mmol) and 4-dimethylaminopyridine (0.001 mg, 0.0.82 mmol). The reaction mixture was stirred under argon for 3 days. After removal of solvents, the residue was purified by column chromatography (silica gel, eluent: acetonitrile (400 mL), NH_4PF_6 (7 g), ethyl acetate (200 mL), cyclohexane (100 mL)). The crude product was washed with water and the residue was dried *in vacuo* to give the product as dark yellow powder (0.144 g, 88%), m.p. 193–195 °C.; $C_{92}H_{100}F_{30}N_5O_8P_5S_2$ (2191.76), calcd (%): C 50.39, H 4.60, N 3.19, S 2.92; found (%): C 50.28, H 4.34, N 3.05, S 2.89;

HRMS (ESI) *m/z*: found 585.5427; calcd for $[M-3PF_6^-]^{3+}$ $[C_{92}H_{100}F_{12}N_5O_8P_2S_2]^{3+}$ 585.5429; found 402.9158; calcd for $[M-4PF_6^-]^{4+}$ $[C_{92}H_{100}F_6N_5O_8PS_2]^{4+}$ 402.9164; found 293.3397; calcd for $[M-5PF_6^-]^{5+}$ $[C_{92}H_{100}N_5O_8S_2]^{5+}$ 293.3401.

Acridane Rotaxane 13. A suspension of **12** (0.100 g, 0.046 mmol) and $NaHCO_3$ (0.150 g) in MeCN (5 mL) and MeOH (0.5 mL) was vigorously stirred for 6 h. After filtration and removal of solvents, the residue was dried *in vacuo* to give the product as colorless oil (0.088 g, 92%). HRMS (ESI) *m/z*: found 901.8196; calcd for $[M-2PF_6^-]^{2+}$ $[C_{93}H_{103}F_{12}N_5O_{10}P_2S_2]^{2+}$ 901.8210; found 552.8914; calcd for $[M-3PF_6^-]^{3+}$ $[C_{93}H_{103}F_6N_5O_{10}PS_2]^{3+}$ 552.8924; found 378.4272; calcd for $[M-4PF_6^-]^{4+}$ $[C_{93}H_{103}N_5O_{10}S_2]^{4+}$ 378.4281.

Acknowledgements

We thank the Deutsche Forschungsgemeinschaft for financial support. We express our sincere thanks to Dr Christian Böttcher (Free University Berlin, Research Centre of Electron Microscopy) for his help in the TEM measurements

Notes and References

1 (*a*) J. F. Stoddart, *Acc. Chem. Res.*, 2001, **34**, 410–411; (*b*) C. A. Schalley, K. Beizai and F. Vögtle, *Acc. Chem. Res.*, 2001, **34**, 465–476; (*c*) V. Balzani, M. Venturi and A. Credi, *Molecular Devices and Machines*, Wiley-VCH, Weinheim, 2003; (*d*) E. R. Kay, D. A. Leigh and F. Zerbetto, *Angew. Chem.*, 2007, **119**, 72–196; *Angew. Chem., Int. Ed.*, 2007, **46**, 72–191.

2 M. C. T. Fyfe, P. T. Glink, S. Menzer, J. F. Stoddart, A. J. P. White and D. J. Williams, *Angew. Chem.*, 1997, **109**, 2158–2160; *Angew. Chem., Int. Ed. Engl.*, 1997, **36**, 2068.

3 W. Clegg, C. Gimenez-Saiz, D. A. Leigh, A. Murphy, A. M. Z. Slawin and S. J. Teat, *J. Am. Chem. Soc.*, 1999, **121**, 4124–4129.
4 (*a*) R. A. Bissel, E. Cordova, A. E. Kaifer and J. F. Stoddart, *Nature*, 1994, **369**, 133–137; (*b*) Y. Jiang, J.-B. Guo and C.-F. Chen, *Org. Lett.*, 2010, **12**, 4248–4251.
5 (*a*) H.-R. Tseng, S. A. Vignon and J. F. Stoddart, *Angew. Chem.*, 2003, **115**, 1529–1539; *Angew. Chem., Int. Ed.*, 2003, **42**, 1491–1495; (*b*) K. Nikitin, E. Lestini, J. K. Stolarczyk, H. Müller-Bunz and D. Fitzmaurice, *Chem.–Eur. J.*, 2008, **14**, 1117–1128.
6 S. Saha and J. F. Stoddart, *Chem. Soc. Rev.*, 2007, **36**, 77–92.
7 (*a*) W. Abraham, K. Buck, M. Orda-Zgadzaj, S. Schmidt-Schäffer and U.-W. Grummt, *Chem. Commun.*, 2007, 3094–3096; (*b*) W. Abraham, A. Wlosnewski, K. Buck and S. Jacob, *Org. Biomol. Chem.*, 2009, **7**, 142–154.
8 (*a*) A. C. Temleton, M. P. Wuelling and R. W. Murray, *Acc. Chem. Res.*, 2000, **33**, 27–36; (*b*) M. C. Daniel and D. Astruc, *Chem. Rev.*, 2004, **104**, 293–346; (*c*) C. Burda, X. B. Chen, R. Narayanan and M. A. El-Sayed, *Chem. Rev.*, 2005, **105**, 1025–1102.
9 (*a*) R. Clajn, J. F. Stoddart and B. A. Grzybowski, *Chem. Soc. Rev.*, 2010, **39**, 2203–2237; (*b*) J. J. Davis, G. A. Orlowski, H. Rahman and P. D. Beer, *Chem. Commun.*, 2010, **46**, 54–63; (*c*) A. Coskun, P. J. Wesson, R. Klajn, A. Trabolsi, L. Fang, M. A. Olson, S. K. Dey, B. A. Grzybowski and J. F. Stoddart, *J. Am. Chem. Soc.*, 2010, **132**, 4310–4320.
10 (*a*) K. G. Thomas and P. V. Kamat, *Acc. Chem. Res.*, 2003, **36**, 888–898; (*b*) E. Dulkeith, A. C. Morteani, T. Niedereichholz, T. A. Klar, J. Feldmann, S. A. Levi, F. C. J. M. van Veggel, D. N. Reinhoudt, M. Möller and D. I. Gittins, *Phys. Rev. Lett.*, 2002, **89**, 203002-1–203002-4; (*c*) A. Manna, P.-L. Chen, H. Akiyama, T.-X. Wie, K. Tamada and W. Knoll, *Chem. Mater.*, 2003, **15**, 20–28.
11 M. Brust, M. Walker, D. Bethell, D. J. Schiffrin and R. Whyman, *J. Chem. Soc., Chem. Commun.*, 1994, 801–802.
12 A. Vetter and W. Abraham, *Org. Biomol. Chem.*, 2010, 4666–4681.
13 R. Ballardini, V. Balzani, M. T. Gandolfi, L. Prodi, M. Venturi, D. Philp, H. G. Ricketts and J. F. Stoddart, *Angew. Chem.*, 1993, **105**, 1362–1364; *Angew. Chem., Int. Ed. Engl.*, 1993, **32**, 1301–1303.